CHAPTER 4

COUPLED FERROELECTRIC E-FIELD SENSOR

Ordinary men look at new things with old eyes.
The creative man observes the old things with new eyes.
- GianPiero Bona

1. INTRODUCTION

This chapter deals with the objective of this Ph. D. thesis. The idea here addressed is the exploitation of ferroelectric material properties and nonlinear dynamics behavior with emphasis on the realization of an innovative transducer.
The focused approach is based on the exploitation of circuits made up by the ring connection of an odd number of elements containing a ferroelectric capacitor, which, when a control parameter (the coupling gain) crosses a threshold value, exhibits an oscillating regime of behavior. For such a device, an external target electric field interacts with the system thus inducing perturbation of the polarization of the ferroelectric material; the target signal can be indirectly detected and quantified via its effect on the system response.
The emergent oscillations occur even in the absence of an applied "target" signal, and their frequency depends on the parameters of each individual element (i.e. the potential energy function when isolated), as

well as the coupling strength. Then, the onset of a quasi-static target signal makes the system asymmetric and leads to changes in the frequency of oscillation, as well as other dynamic characteristics [137]. These changes are used to quantify the symmetry-breaking signal, i.e. the amplitude of the target electric field.

The conceived devices exploit the synergetic use of bistable ferroelectric materials, micromachining technologies that allow us to address charge density amplification, and implement novel sensing strategies based on coupling non-linear elemental cells.

Simulation results have shown that for a coupling factor (related to the external field strength), between the ring cells greater than the critical one, a change in the harmonic content of the permanent oscillations generated in the coupled system occurs.

Advanced simulation tools have been used for modeling a system including electronic components and non linear elements as the conceived micro-capacitors. Moreover, Finite Element Analysis (FEM) has allowed us to steer the capacitor electrodes design toward optimal geometries and to improve the knowledge of effects of the external target E-field on the electric potential acting on the ferroelectric material.

An experimental characterization of the whole circuit, including three cells coupled in a ring configuration has also been carried out in this case. The results confirm the increasing of the circuit oscillation frequency as a function of the coupling factor, as expected from the mathematical and numerical models. A theoretical development of the underlying dynamics has also been given in [138].

The theory underpinning the non linear dynamic system as well its modeling and description together with the experimental results will be faced in the next sections.

2. OSCILLATIONS IN UNIDIRECTIONALLY COUPLED OVERDAMPED BISTABLE SYSTEMS

Overdamped unforced dynamical systems do not oscillate. However, well-designed coupling schemes, together with the appropriate choice of

initial conditions, can induce oscillations when a control parameter exceeds a threshold value [137], [139].

Previous investigations [140], [141] showed that $N \geq 3$ (odd) unidirectionally coupled elements with cyclic boundary conditions and ensuring that at least one of them has an initial state that is different from the others would, in fact, oscillate when a control parameter - in this case the coupling strength - exceeded a critical value. The characteristics of the bifurcation to oscillatory behavior depend on the system dynamics and, more importantly, the manner in which the elements are coupled [139]. These oscillations are now finding utility in the detection of very weak target E-field signals, via their effect on the oscillation characteristics.

Overdamped bistable dynamics, of the generic form

$$\dot{x} = -\nabla U(x) \tag{4.1}$$

underpin the behavior of numerous systems in the physical world. The most studied example is the overdamped Duffing system: the dynamics of a particle in a bistable potential

$$U(x) = -ax^2 + bx^4 \tag{4.2}$$

Frequently, bistable systems are also characterized by a “soft” potential (to be contrasted with the “hard” Duffing potential which approaches $\pm\infty$ far more steeply) consisting of a nonlinear addition to a parabolic component, the latter being, of course, characteristic of linear dynamics. Among these systems it is surely possible to number the dynamics of hysteretic ferromagnetic cores (treated as a macroscopic single domain entity) [140] as well the dynamics of hysteretic ferroelectric capacitors [142], [143]. Absent an external forcing term, the state point $x(t)$ will rapidly relax to one of two stable attractors, for any choice of initial condition. The latter statement is depicted in Figure 4-1. More details on this picture will be given in section 3.2. This behavior is, of course, universal in overdamped dynamical systems.

For the case of Duffing dynamics with additive inter-element coupling [141], the system undergoes a Hopf bifurcation to oscillatory behavior; the oscillation frequency is nonzero infinitesimally past the bifurcation point, and increases as one goes deeper into the bifurcation

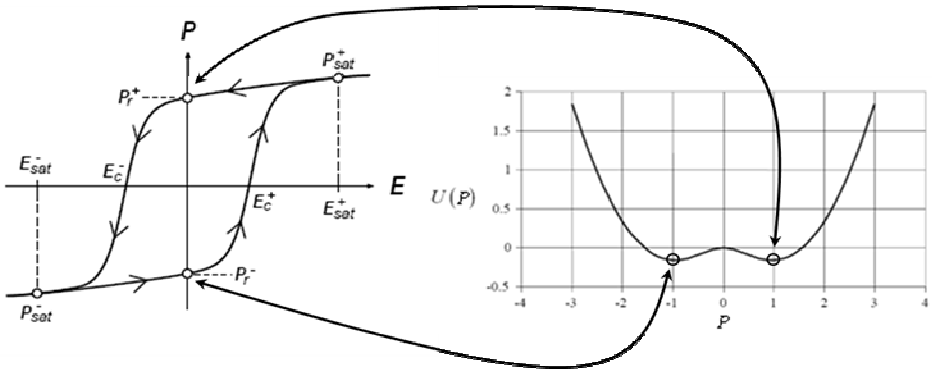

(a) (b)

FIGURE 4-1 (a) Ferroelectric hysteresis loop, and, (b) the corresponding potential energy function that underpins the dynamics.

regime. Figure 4-2 shows the effect of coupling and how oscillations are generated once the coupling parameter reaches a critical value [144] [145]. Global bifurcation occurs at λ_c, the critical coupling. Figure 4-2 shows the behavior of a coupled system for oscillation. Here, a potential well function derived from a coupled system of equations vs the coupling parameter, λ_c, is plotted. As shown, for no coupling ($\lambda = 0$) the potential function is symmetric, and the solutions (shown as spheres in Figure 4-2) remain in steady state or single potential well. Once coupled, the system begins to oscillate for $\lambda > \lambda_c$. For nonzero coupling below the critical coupling, $\lambda < \lambda_c$, the system becomes asymmetric, but does not switch between the potential wells. At the critical value (global bifurcation) the dynamics of the coupled system change and switching occurs. Above the critical coupling the system is in the self oscillating or supercritical regime hence the oscillation between potential wells begin when $\lambda > \lambda_c$. This behavior is induced without an input signal function [144].

In [141], this property was exploited in a simple model of two interacting neural "columns," and shown to lead to the appearance of certain well-characterizable frequency components in the response.

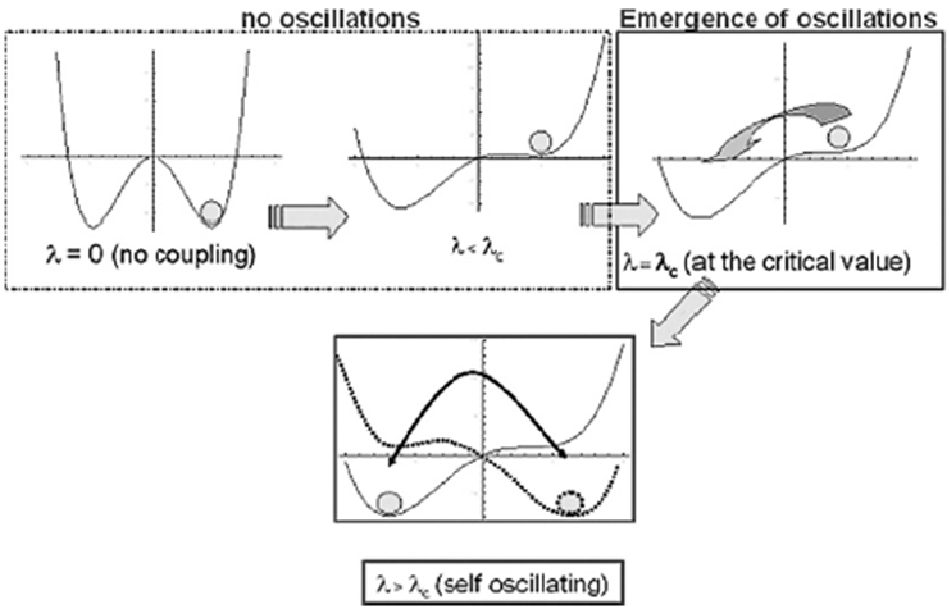

FIGURE 4-2 Oscillations: potential well function vs. the coupling λ.

In [137] a system of coupled elements having "soft"-potential dynamics, characteristic of hysteretic single-domain ferromagnetic cores, has been considered.

This work has led to exploiting the emergent oscillatory behavior for signal detection purposes: specifically, an external symmetry-breaking dc magnetic signal having small amplitude (usually much smaller than the energy barrier height of a single element) can be detected and quantified via its effect on the oscillation frequency and asymmetry of the oscillation wave forms.

This last work has inspired this thesis [142].

3. THE ELEMENTARY CELL AND THE SENSING STRATEGY

As previously stated the system here addressed consist in a circuit made up by the ring connection of an odd number of non linear dynamical elements. Each active element is essentially realized by a micromachined capacitor whose core is a ferroelectric material that can be polarized through an imposed driving field and the conditioning electronics. Coupling between contiguous cells take place by gain blocks (from which depends the coupling strength) which, essentially consist in non inverting amplifier; more details will be given in section 6.1.

Figure 4-3 shows the schematic of the single non linear cell: it consist in a ferroelectric capacitor C_{FE} and a Sawyer-Tower conditioning circuit. A third electrode (ΔP) in the ferroelectric capacitor, hereinafter "the sensing electrode" allows to alter the polarization state when the target electric field is applied, resulting in a distortion of the polarization vs. electric field hysteresis loop. In addition, a suitable external receptor, hereinafter "the charge collector" (not shown in Figure 4-3), allows for amplification of the target field to the sensing element.

In the following, both the ferroelectric capacitor and the conditioning circuit will be discussed.

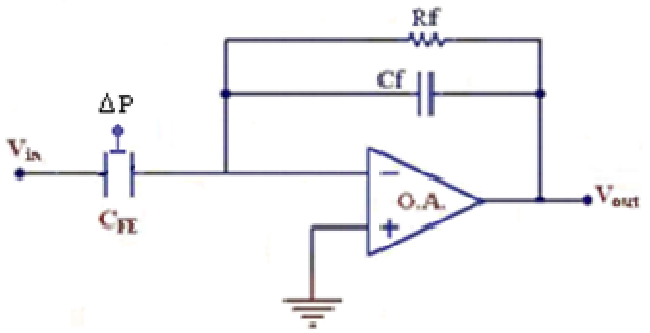

FIGURE 4-3 Schematic of the Sawyer-Tower conditioning circuit where the "sensing" electrode in the CFE capacitor, used to induce the perturbation ΔP in the ferroelectric polarization status, is highlighted.

3.1. THE FERROELECTRIC CAPACITOR AND THE CONDITIONING CIRCUIT

Since they were introduced as storage elements in integrated nonvolatile memory applications, ferroelectric capacitors have aroused remarkable interest for its potential applications.

In this work it plays the central rule of sensing element. For a better understanding on how we want use the capacitor to sense an external electric field E_x a schematization of the ideal structure of the capacitor is given in Figure 4-4. It is a parallel-plate capacitor having as dielectric a ferroelectric material and hosting in the upper electrode a third separated central electrode, the sensing electrode (the electrode marked as ΔP in Figure 4-3), used to convey the perturbation (due to the target field) to the sensing region. The latter electrode is wired to a "charge collector" consisting of a copper plate. The purpose of the "charge collector" is to collect the charges induced by the target electric field; in turn, the collected charge is immediately transferred to the sensing plate thus perturbing the polarization of the ferroelectric material. The bottom and the upper outer electrodes (the driving electrodes) are used to produce a bias polarization in the ferroelectric.

The readout strategy utilizes a Sawyer-Tower (ST) circuit [146] shown in Figure 4-3 where C_{FE} and C_f represent the ferroelectric capacitor (with the sensing electrode to induce a perturbation ΔP in the ferroelectric polarization status, schematically shown) and the feedback capacitor respectively, while R_f was introduced to avoid the drift in the circuit output. Effectively, the ST circuit is a charge integrator which, by a charge to voltage conversion, permits the measurement of the average polarization in the material. The frequency response of the ST circuit is given by:

$$G(s) = \frac{V_{out}(s)}{V_{in}(s)} = -\frac{C_{FE}}{C_f}\frac{sC_f R_f}{(1+sC_f R_f)} \tag{4.3}$$

Choosing an appropriate value (in the frequency domain, s denoting the frequency) for R_f ($R_f >> 1/sC_f$) leads to

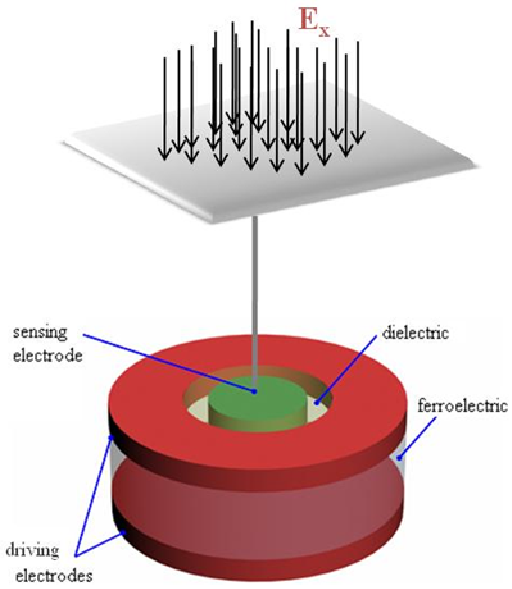

FIGURA 4-4 Schematization of the structure of the ferroelectric capacitor used to sense an external electric field E_x. It is a parallel-plate capacitor having as dielectric a ferroelectric material and hosting in the upper electrode a third separated central "sensing" electrode used to convey the charges induced by the target electric field on the "charge collector" to the ferroelectric. The bottom and the upper outer driving electrodes are used to produce a bias polarization in the ferroelectric.

$$V_{out} = -\frac{A_{FE}}{C_f} P \tag{4.4}$$

with A_{FE} and P being the areas of the driving electrodes of the ferroelectric capacitor and the material polarization, respectively. The driving voltage V_{in} is related to the applied electric field E and the material thickness d by

$$V_{in} = Ed \tag{4.5}$$

The ST circuit operates in a high-pass mode: in order to suitably stimulate the ferroelectric capacitor a constant target E-field must be

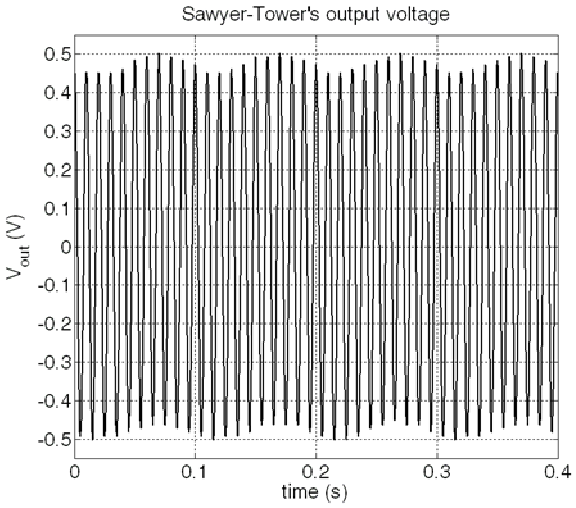

FIGURA 4-5 A typical Sawyer-Tower output voltage signal where the amplitude modulation of the reference signal is a result of the applied (target) low frequency signal.

modulated into a quasi-static signal and this can be accomplished via a field-mill strategy. In the remainder of the thesis a low frequency external electric field will be used for experimental characterization purposes. An example of a typical ST output is shown in Figure 4-5; in this figure, the "amplitude modulation" of the reference driving signal (applied in order to overcome the coercive field and induce hopping events between the stable steady states of the potential) due to a (low frequency) target electric field is clearly visible.

3.2 A MODEL FOR THE FERROELECTRIC CAPACITOR

To the purpose to implement the coupled configuration it is mandatory to define an analytical model for the ferroelectric capacitor with the sensing electrode and then to characterize the behavior of the elementary cell. This latter step focuses on the characterization of the previous circuit as single E-field sensor and will be faced hereinafter in section 5.

There have been many attempts at modeling the behavior of hysteretic materials and ferroelectric capacitors [147], [148], [149], [150], [151], [152]. Several models aimed at predicting the behavior of hysteretic devices are present in the literature, e.g. the *state space model* [153], the *viscoelastic model* [154], the *tanh* model [155], the *Preisach model* [156], [157], while many other models have been developed to address ferroelectric capacitors [152], [158], [159]. A significant analytical representation of the macroscopic dynamic behavior in a ferroelectric sample can be realized by the *Landau-Khalatnikov equation* [160]

$$\tau \frac{dP}{dt} = -\frac{\partial U(P,t)}{\partial P} \tag{4.6}$$

where P is the electric polarization and τ the system time constant. This model describes the hysteretic behavior via the (bistable) potential energy function *U(P,t)* which underpins the switching mechanism between the two stable states of the system. An example of the potential is given in the Figure 4-1, together with its correspondence with the hysteresis loop. The height of the potential barrier represents the energy required to switch from one stable state to the other under a static applied electric field. We adopt (following the Landau-Khalatnikov model) a "standard quartic" form for the potential,

$$U(P,t) = -\frac{a}{2}P^2 + \frac{b}{4}P^4 - cE(t)P \tag{4.7}$$

which yields the dynamic model

$$\tau \dot{P} = aP - bP^3 + cE(t) \tag{4.8}$$

where a, b, c and τ are quantities to be estimated. In particular, a and b are material dependent, c is a fitting parameter and τ is a time constant which rules the dynamic behavior of the system, while *E(t)* represents the driving field. As will be discussed in the next sections, the ideal driving signal, *E(t)*, would have an amplitude just above what is necessary to overcome the coercive field of the material. The overdot denotes (throughout this work) the time-derivative.

The presence of a target signal results in the asymmetry of *U(P,t)*, and detection techniques are aimed at quantifying this asymmetry. In this case the electric field *E* is the result of the contributions coming from an auxiliary electric field (the driving field) and from an external electric field (the target field); it is this target field that modifies the oscillation characteristic of the network in the case of the coupled system.

3.3 THE CHARGE COLLECTION STRATEGY

The methodology, proposed here, to sense a quasi-static electric field can be synthesized through the following relationship:

$$\Delta E_x \rightarrow \Delta P \rightarrow \Delta V_{0ut} \tag{4.9}$$

Put simply, a variation of the target electric field produces a concomitant variation in the polarization state of the ferroelectric layer in the sensing region; in turn, this change in polarization is transduced into a voltage variation by the conditioning circuit, as indicated in (4.4). Naturally the first part ($\Delta E_x \rightarrow \Delta P$) of (4.9) must be modeled and validated. An analytic model describing the relation between the target electric field and the polarization in the ferroelectric related to the dimensions of the charge collector is now presented.

Let us consider the model system consisting of two large electrodes used to generate the target electric field (the exact experimental setup will be described in section 5.1.6), the charge collector, and the ferroelectric capacitor. This system can be represented by two parallel plate capacitors connected in a series configuration as indicated in Figure 4-6, where C_1 represents the capacitors formed by the large electrode and the charge collector and C_2 the ferroelectric capacitor under the sensing electrode. Denoting S_1 as the area of the charge collector and assuming a symmetrical distribution of the charge Q on the plates of capacitors, we obtain as a natural result of Gauss' law

$$\sigma_1 = \frac{Q}{S_1} = \varepsilon_0 \cdot E_x \tag{4.10}$$

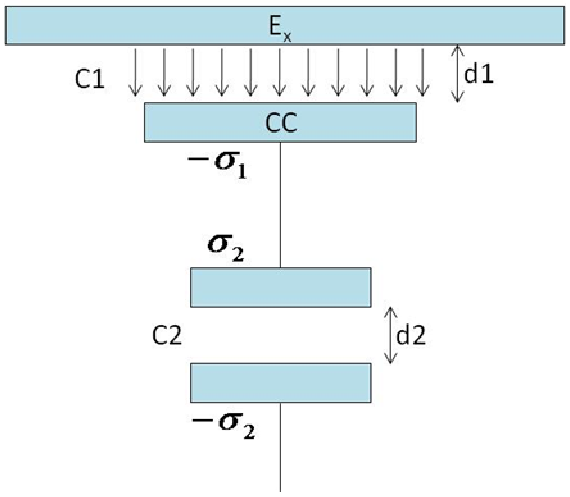

FIGURA 4-6 A schematization of the charge collection strategy.

where σ_1 is the charge density on the surface of an electrode of C_1. This configuration readily leads to

$$\sigma_2 = \frac{Q}{S_2} = \frac{S_1}{S_2} \cdot \varepsilon_0 \cdot E_x \tag{4.11}$$

where S_2 and σ_2 represent the surface area of the sensing electrode of capacitor C_2 and its charge density, respectively.
Now, considering that, for weak perturbations, the relationship between polarization and the dielectric displacement vector is given by

$$D = P + \varepsilon_0 E_{pol} \tag{4.12}$$

and assuming the polarization field to be close to zero in the vicinity of the sensing electrode ($E_{pol} \cong 0$) for C_2, it follows that $P = D = \sigma_2 \vec{u}_n$, with $\vec{u}_n$ representing the normal vector to the surface S_2. As a direct consequence we obtain,

$$\Delta P = \Delta\sigma_2 = \varepsilon_0 \frac{S_1}{S_2} \Delta E_x \tag{4.13}$$

Hence, the perturbation in the polarization state of the ferroelectric material is directly related to the external target field and this effect is

amplified by the ratio between the two plate areas. These theoretical results will be experimentally verified in section 5.1.6.
Equation (4.13) relates the polarization of the ferroelectric material with the target electric field via the ratio of the surface areas of the charge collector and the sensing electrode. It asserts that a variation of the target electric field yields a proportional variation in the polarization state of the ferroelectric region under the sensing electrode and, hence, a variation of the output voltage of the conditioning circuit. This behavior can be modeled by modifying equation (4.8) as follows:

$$\tau \dot{P} = a\,(P + \Delta P) - b\,(P + \Delta P)^3 + cE(t) \tag{4.14}$$

4. THE COUPLED CIRCUIT

The coupled circuit consist on a ring connection of an odd number of elementary cells. Figure 4-7 shows an example of coupled circuit with $N = 3$ elementary cells. The unidirectional coupling between contiguous cells is obtained by gain blocks (K-blocks in Figure 4-7) whose circuital implementation will be discussed in section 6.1.
Let us to consider the first cell, it is easy to write the following equation for the electric field E_1 on the ferroelectric capacitor:

$$E_1 = \frac{V_{in1}}{d} = \frac{V_{out3} K}{d} \tag{4.15}$$

where d represents the thickness of the dielectric in the capacitor (the ferroelectric material), V_{in1} and V_{out3} the voltage applied to the ferroelectric capacitor and the output voltage of the third cell, respectively and K the gain of the coupling block between the third and the first cell.
Taking in account equation (4.4) it follows

$$E_1 = -\frac{A_{FE}}{C_f d} K P_3 \tag{4.16}$$

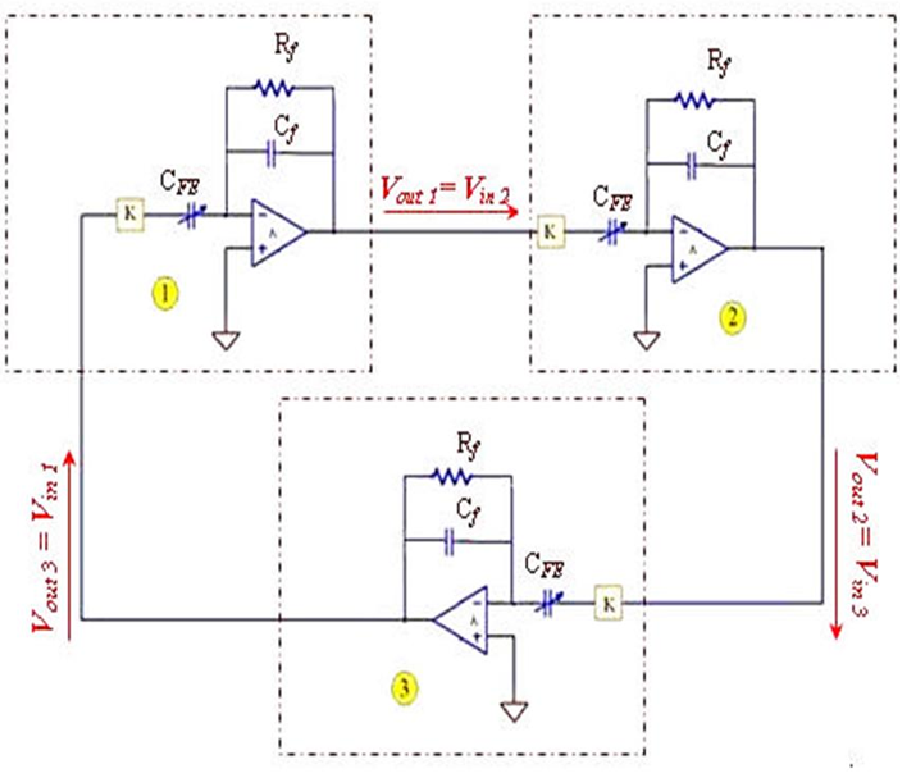

FIGURA 4-7 Schematization of the coupled circuit with N=3 elementary cells.

Sitting equation (4.16) in (4.8) it follows for the first elementary cell

$$\tau \dot{P}_1 = aP_1 - bP_1^3 + cE_1 = aP_1 - bP_1^3 - c\frac{A_{FE}}{C_f d}KP_3 \tag{4.17}$$

and setting

$$\lambda = c\frac{A_{FE}}{C_f d}K \tag{4.18}$$

it readily follows

$$\tau \dot{P}_1 = aP_1 - bP_1^3 - \lambda P_3 \tag{4.19}$$

The parameter λ represents the coupling coefficient between contiguous cells. The coupled circuit can oscillate if the coupling strength exceeds a critical value ($\lambda > \lambda_c$)

$$\lambda_c = \frac{a}{2} + \frac{3}{2}\frac{cE_x}{1+\sqrt{\frac{2a}{b}}} \tag{4.20}$$

where E_x is the external target electric field. It follows that for the coupling circuit, when no external electric field is present, the critical value $\lambda_c = a/2$.

A dependence of the oscillation frequency of the circuit from the coupling coefficient as been theoretically predicted [137], [139] and experimentally observed (see section 6.1).
Writing equation (4.19) for the other two cells we obtain the set of equations modeling the coupling system in Figure 4-7

$$\begin{cases} \tau \dot{P}_1 = aP_1 + bP_1^3 - \lambda P_3 \\ \tau \dot{P}_2 = aP_2 + bP_2^3 - \lambda P_1 \\ \tau \dot{P}_3 = aP_3 + bP_3^3 - \lambda P_2 \end{cases} \tag{4.21}$$

In this set of equations as been implicitly assumed that the three ferroelectric capacitors in the coupled cells are exactly alike, therefore the parameters a, b and λ (which depends even from the parameter c) are considered to be identical.
In fact, due to the technology tolerances, the capacitors could not be exactly alike and a different set of parameters for the single capacitor should be taken in account.
In the same way as in the single elementary cell, the effect of an external target E-field can be taken in account modifying the set of equations (4.21). Here more than one configurations can be investigated if we consider the possibility to connect the charge collector to one single or more ferroelectric capacitors in the circuit. In the simple case in which the charge collector is connected to a single capacitor in the ring coupled circuit (for example the capacitor of the third cell) it follows

$$\begin{cases} \tau \dot{P}_1 = aP_1 + bP_1^3 - \lambda P_3 \\ \tau \dot{P}_2 = aP_2 + bP_2^3 - \lambda P_1 \\ \tau \dot{P}_3 = a(P_3 + \Delta P) + b(P_3 + \Delta P)^3 - \lambda P_2 \end{cases} \tag{4.22}$$

the variation of the polarization ΔP due to the target electric field has to be taken in account only in the capacitor directly connected to charge collector. However, as we will see experimentally, the effect of the target field propagates in the circuit, affecting the output voltage of every cell in the circuit.

5. INVESTIGATION OF THE SINGLE CELL AS E-FIELD SENSOR

In section 3.2 it has been stated that to the aim to implement the coupled configuration it is mandatory to define an analytical model for the ferroelectric capacitor with the sensing electrode and then to characterize the behavior of the elementary cell. The former issue has been faced in part in the same section. In this section this model will be used to match experimental data to the purpose to characterize the behavior of the ferroelectric capacitor. Moreover the investigation and characterization of the capacitor with the conditioning ST circuit (see Figure 4-3) as single E-field sensor will be discussed together with experimental evidences.

Experiments with three types of ferroelectric capacitors have been carried out and will be discussed in the sequel.

To verify the correctness of the proposed methodology and for the sake of design a behavioral model of the device is mandatory. Figure 4-8 depicts the schematization of the work flow required to simulate the behavior of the ferroelectric sensor.

The first task to be performed is the identification of model (4-8) which, as an example, can be achieved by the Nelder-Mead optimization algorithm [161].

To the purpose of modelling the effect of the external target field (E_x) on the device polarization (ΔP) a Finite Element Analysis of the device

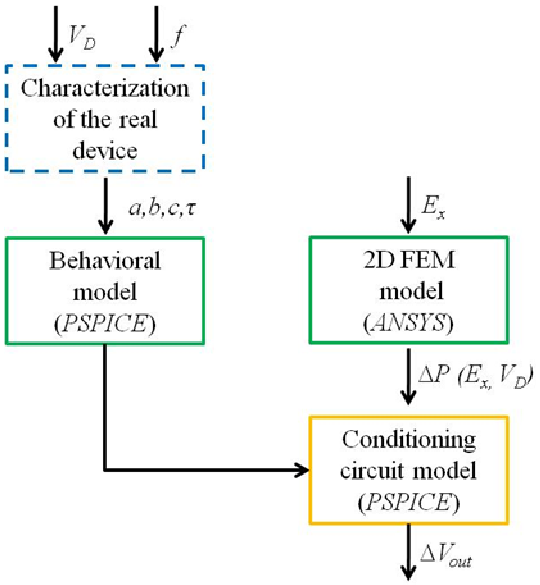

FIGURE 4-8 Schematization of the work flow required to simulate the behavior of a ferroelectric sensor.

behavior can be performed. In Section 5.1.1, an approach based on the *ANSYS* environment will be discussed.

Once the model parameters and the relationship between E_x and ΔP are known, it would be interesting to implement an electric model in *PSPICE* to simulate the electric behavior of the device also in a Sawyer-Tower configuration and in the presence of an external field. This task will be investigated in Section 5.1.4.

5.1 THE PENN STATE CAPACITOR

First experiments have been conducted with ferroelectric capacitors preliminarily realized at the Penn State University. Starting from a silicon substrate a common silver electrode has been evaporated, the ferroelectric material has been deposited over the bottom electrode, and finally several top electrodes have been spotted over the top surface of the ferroelectric in order to realize both the capacitors, and the external connections. Figure 4-9 shows (a) a real view of the prototypes used here

together with a detailed view of the material layers, (b) a microscope picture of the ferroelectric sample and (c) a schematic of the bonding between the plates of the capacitors and the pins of the hosting package, respectively.

The structure of these capacitor does not mirror the ideal structure previously introduced in section 3.1 and shown in Figure 4-4. To the purpose to mimic the desiderated structure the configuration shown in Figure 4-10 has been adopted. The ferroelectric capacitor considered here consists (from bottom to top) of a common bottom electrode, a thin layer of ferroelectric material, and a pair of driving electrodes (producing the bias polarization) hosting a central sensing electrode. The capacitor polarization is induced via the voltage applied to the driving electrodes, with the charges accumulated in the sensing electrode producing a perturbation to the polarization state.

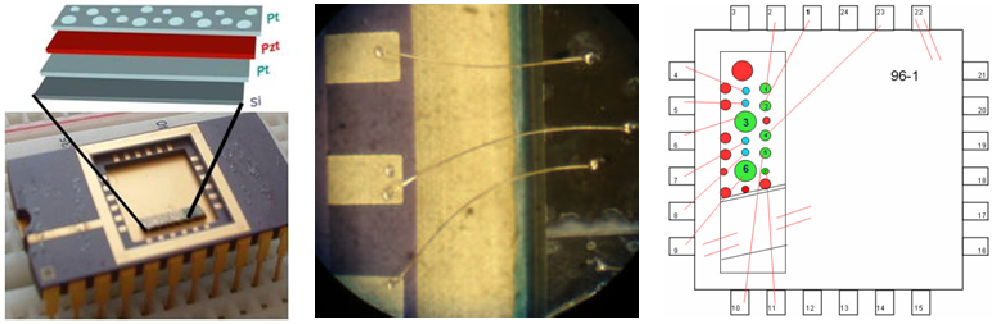

(a) (b) (c)

FIGURE 4-9 The Penn State ferroelectric capacitor: (a) a real view of the prototypes together with a detailed view of the material layers, (b) a microscope picture of the ferroelectric sample and (c) a schematic of the bonding between the plates of the capacitors and the pins of the hosting package.

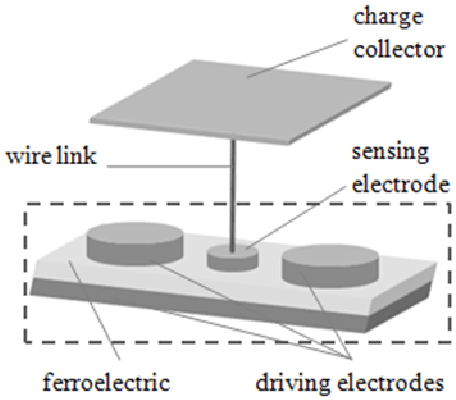

FIGURE 4-10 Device schematic wherein the dashed line outlines the ferroelectric capacitor in which two large top driving electrodes are used to polarize the ferroelectric "sensing region". The small electrode in the middle ("the sensing electrode") is wired to a "charge collector" that collects the charges induced by the target electric field.

The electrodes are made of platinum while the ferroelectric layer, with a thickness of 2.17 μm, has a composition of 30/70 PZT with a 20% excess of Pb.
The idea is to use a three-electrode configuration: two medium or large electrodes to polarize a region of the ferroelectric layer (the sensing region) and a small electrode, placed in the same region, to convey the perturbation (due to the target field) to the sensing region.
This behavior has been confirmed via FEM analysis [73],[144] and will be discussed in the following section.

5.1.1 ANSYS SIMULATIONS

A 2D model has been developed to investigate the relationship between the target E-field and the variation of polarization in the ferroelectric material [162].
Two main steps are fundamental for the quality of results: the definition of the device geometry and the meshing. The latter must follow some basic rules and must be generated in a proper way to avoid bad results or an overgrowing need of computational power. This can be

achieved with a careful choice of the meshing element and a gradual change in mesh dimensions along areas of different interest. Figure 4-11 illustrates some examples of meshes adopted to simulate the behavior of the device under consideration. In particular, Figure 4-11a shows a view of the area including the sensor and the shielding box with the charge collector, while Figure 4-11b is a zoom of the sensor area.

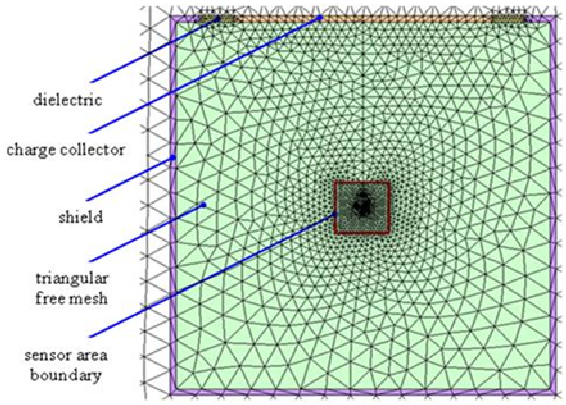

(a)

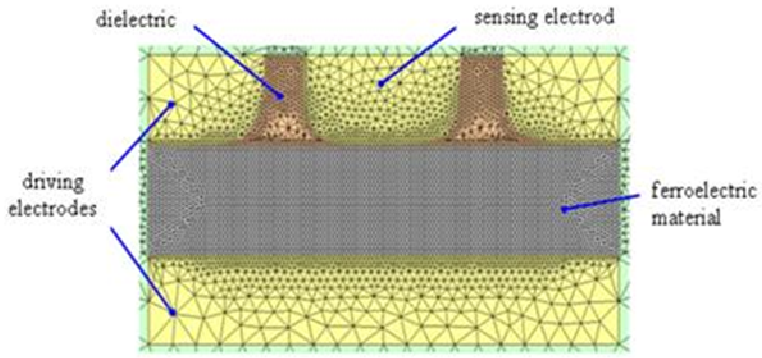

(b)

FIGURE 4-11 A view of the meshed device including a shielding chamber and the charge collector (a), and a zoom of the sensor region (b).

Figure 4-12 shows results of a typical FEM simulation: the polarization state of the cross section is shown without (Figure 4-12a) and with (Figure 4-12b) a perturbing action produced through the sensing electrode. Actually, the amplitudes of the vertical component of the polarization vector in the ferroelectric capacitor is given for a device polarized with a standard driving voltage and in the presence of a low value of the external target E-field.

The changes induced in the polarization status of this capacitor will manifest themselves in alterations of the output signal from the signal conditioning circuit.

From the FEM simulations it is possible to obtain the relationship between a variation of the external target field and the corresponding perturbation of the polarization, ΔP.

This relationship is strategic for the sake of simulating the sensor behavior in the *PSPICE* environment. Following the work flow in Figure 4-7, to this aim the identification of model (4.8) is mandatory. To this purpose a characterization of the device behavior in the P-E domain, varying the amplitude and frequency of the driving voltage, has been performed and will be discussed in the next section.

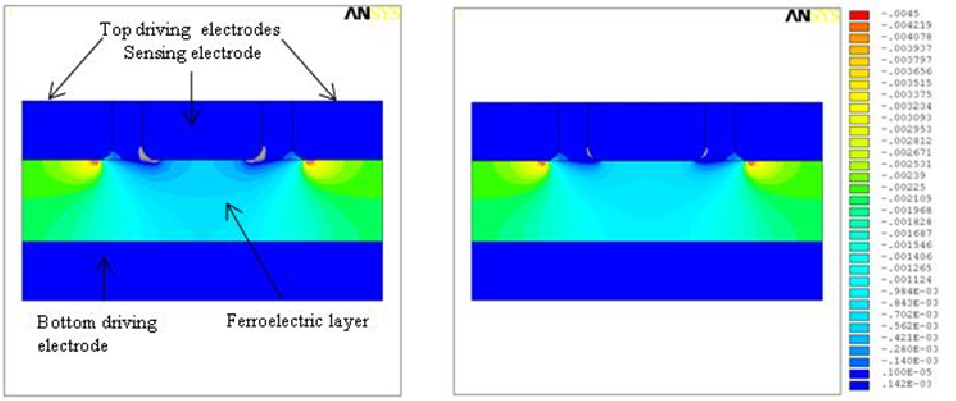

(a) (b)

FIGURE 4-12 Qualitative FEM analysis of the ferroelectric capacitor without (a) and with (b) a perturbing action produced through the sensing electrode